第 27 卷第 5 期 无 机 化 学 学 报 Vol.27 No.5
2011 年 5 月 CHINESE JOURNAL OF INORGANIC CHEMISTRY 1008-1014

玫瑰花状多孔碱式碳酸镁微球的合成

宋兴福* 杨 晨 汪 瑾 孙淑英 于建国
(国家盐湖资源综合利用工程技术研究中心华东理工大学,上海 200237)

摘要:介绍了一种便利的玫瑰花状多孔碱式碳酸镁($4MgCO_3\cdot Mg(OH)_2\cdot 4H_2O$)微球的合成方法,该方法分为三水碳酸镁($MgCO_3\cdot 3H_2O$)前驱物合成与其在水中的热解制备过程。采用搅拌诱导结晶辅助陈化的方法合成前驱物,得到长约 115 μm,长径比约 10.4 的均一微棒,将微棒在 353.2 K 的水中热解,即可得到由弯曲的纳米片组成的具有"卡片箱"结构(house of cards)的玫瑰花状多孔碱式碳酸镁微球,微球直径为 30~60 μm,平均约 40 μm,具有良好分散性。研究了热解过程中的形貌转变和相转移过程,采用 XRD,FTIR 及 SEM 表征样品的结构和形貌。结果表明:$MgCO_3\cdot 3H_2O$ 在较高温度下因不稳定而溶解,形成局部过饱和,生成无定形颗粒,并在微棒上成核结晶为 $4MgCO_3\cdot Mg(OH)_2\cdot 4H_2O$ 纳米片。纳米片由与微棒附着部位向外生长,形成玫瑰花状微球,微球长大伴随微棒的消溶,生长在棒上不同部位的颗粒在微观结构上将留有不同痕迹。分析认为热解转变过程是($MgCO_3\cdot 3H_2O$)溶解–无定形物生成-($4MgCO_3\cdot Mg(OH)_2\cdot 4H_2O$)结晶的过程。

关键词:三水碳酸镁;碱式碳酸镁;形貌;热解
中图分类号:O614.22;TQ132.2 **文献标识码**:A **文章编号**:1001-4861(2011)05-1008-07

Synthesis of Porous Hydromagnesite Microspheres with Rosette-Like Morphology

SONG Xing-Fu* YANG Chen WANG Jin SUN Shu-Ying YU Jian-Guo
(*National Engineering Research Center for Integrated Utilization of Salt Lake Resource, East China University of Science and Technology, Shanghai* 200237, *China*)

Abstract: Porous hydromagnesite ($4MgCO_3\cdot Mg(OH)_2\cdot 4H_2O$) microspheres with rosette-like morphology were synthesized by a facile pathway. The procedure involved the synthesis of nesquehonite ($MgCO_3\cdot 3H_2O$) precursor and its pyrogenation in water. $MgCO_3\cdot 3H_2O$ precursors were synthesized via a stirring-induced crystallization method assisted by aging. Uniform rod-like precursor could be obtained with a length of about 115 μm and aspect ratio of about 10.4. $4MgCO_3\cdot Mg(OH)_2\cdot 4H_2O$ porous microspheres with "house of cards" structure composed of curly nano-sheets crystals were obtained via the pyrogenation of $MgCO_3\cdot 3H_2O$ in water at 353.2 K. The diameter of hydromagnesite spheres is in the range of 30~60 μm and 40 μm in average with well dispersity. Shape evolution and phase transfer during the transformation were studied by time-evolution experiments. The synthesized samples were characterized by XRD and FTIR as well as SEM. The results show that $MgCO_3\cdot 3H_2O$ dissolves and local supersaturation is formed. Amorphous particles are produced and crystallized into $4MgCO_3\cdot Mg(OH)_2\cdot 4H_2O$ nanosheets on the microrods. Hydromagnesite nano-sheets grow outward from the attachment site forming porous rosette-like microspheres. A mechanism form $MgCO_3\cdot 3H_2O$ microrods to $4MgCO_3\cdot Mg(OH)_2\cdot 4H_2O$ microspheres is suggested to be ($MgCO_3\cdot 3H_2O$) dissolution-amorphous particles formation-($4MgCO_3\cdot Mg(OH)_2\cdot 4H_2O$) crystallization.

Key words: nesquehonite; hydromagnesite; morphology; pyrogenation

收稿日期:2010-08-24。收修改稿日期:2011-01-21。
上海市自然科学基金(09ZR147900),中央高校基本科研业务费专项基金,教育部新世纪优秀人才计划(NCET-08-0776)和上海市重点学科建设(No.B506)资助项目。
*通讯联系人。E-mail:xfsong@ecust.edu.cn

0 Introduction

The properties of particles are often closely correlated to their shapes[1-4]. Functional inorganic materials with diverse morphologies are utilized in many fields[5-8]. There have been increasing interests in designing and fabricating desirable micro- and meso-inorganic materials[9-12].

Hydromagnesite or basic magnesium carbonate $4MgCO_3 \cdot Mg(OH)_2 \cdot 4H_2O$, as one of the most important minerals in geology and planetlogy[13], can be used as fire retardant as well as the carrier and precursor for other magnesium-based chemicals. Moreover, it is widely used in the area of food, pharmaceutical, pigments and daily necessities[14]. As a monoclinic crystal, $4MgCO_3 \cdot Mg(OH)_2 \cdot 4H_2O$ exhibits hexagonal plate-shaped characteristics. However, due to its self-assembly properties, plate-like microcrystal will gather together. The form of spherical, rose-like, nest-like, tubular particles and other forms are the results of self-assembled hydromagnesite nano-sheets.

Hydromagnesite morphology is varies with synthesis ways. Du et al.[15] used $Mg(NO_3)_2$ with pH value of 7.5 and Na_2CO_3 as raw materials to react at 353.2 K to obtain $4MgCO_3 \cdot Mg(OH)_2 \cdot 4H_2O$ micro-rods with a surface of "house of cards" structure. Mitsuhashi and co-workers[16] synthesized needle-like $MgCO_3 \cdot 3H_2O$ at 318 K, and obtained tubular $4MgCO_3 \cdot Mg(OH)_2 \cdot 4H_2O$ crystals with a "house of cards" structure by controlling the operation conditions. They also prepared petaloid hydromagnesite microspheres under ultrasonic irradiation[17]. Zhang et al.[18] prepared basic magnesium carbonate by double carbonation under atmospheric pressure and studied the influences of different pyrogenation temperatures and different additives on the crystal morphology. Cheng et al. and Li et al.[19-20] evaluated the effects of supersaturation and temperature on the preparation of magnesium carbonate hydrates. Recently, the synthesis of spherical or nest-like $4MgCO_3 \cdot Mg(OH)_2 \cdot 4H_2O$ is mainly conducted through the reaction crystallization method[21] or hydrothermal method[22-24] by mixing soluble magnesium salt and carbonate salt under certain conditions.

Direct precipitation method will result in a close packing "stack" structure constructed by nanosheets. While porous "house of cards" structure can only be obtained through rod-like nesquehonite transformation and high purity hydromagnesite will be obtained with pre-washed rods as the precursor. Among the factors affecting the morphology of hydromagnesite, the precursors size is particularly important. Larger particles can provide enough supersaturation and growth material to form a complete spherical shape. If the precursor particles are very small, only aggregates consisted of few flakes can be obtained. We report here a facile pathway to synthesize $4MgCO_3 \cdot Mg(OH)_2 \cdot 4H_2O$ by pyrogenation process as well as a method to prepare suitable nesquehonite precursor.

1 Experimental

All chemicals used were analytical grade (Shanghai Lingfeng Chemical Reagent Co., Ltd.) and used without further purification. Water used was deionized water. The $MgCO_3 \cdot 3H_2O$ precursor was prepared by mixing $MgCl_2$ with Na_2CO_3 solution at 293.2 K and then taken as the reagent. $MgCl_2$ solution (0.50 mol·L^{-1}, 160 mL) was placed in a glass jacket crystallization reactor at 293.2 K. Subsequently, Na_2CO_3 solution (0.50 mol·L^{-1}, 160 mL) was rapidly added into the vigorously stirred crystallization reactor within 3~4 s. The mixture was further stirred for 15 min with constant mechanical stirring rate and the temperature was maintained at 293.2 K for 6 h under static conditions. The white precipitate was collected and filtered off, washed with ethanol for several times and then placed in an oven at 333.2~353.2 K for about 5 h to give the nesquehonite precursor. The spherical hydromagnesite was obtained from nesquehonite via pyrogenation process. At this stage, 100 mL deionized water was heated to 353.2 K. Then 1.0 g $MgCO_3 \cdot 3H_2O$ synthesized was added into the deionized water under stirring. Soon afterwards, the agitation was stopped rapidly. The sample dispersed at the bottom of the reactor and the temperature was maintained at 353.2 K for 3 h. After that, the precipitate was collected and filtered off, washed with ethanol for several times and then

dried in an oven at 353.2 K overnight to obtain the target product hydromagnesite.

XRD patterns were recorded on a D/MAX 2550 VB/PC, using Cu $K\alpha$ radiation, λ=0.154 18 nm, operating at 40 kV, 100 mA and scanning rate at 12°·min^{-1} from 5° to 75°.The fourier transform infrared spectra (FTIR) were recoded on Nicolet 6 700 (KBr Pellets method). The morphology and particle size of the as-synthesized samples were examined by a scanning electron microscopy (SEM, JEOL-JSM-6700F, 15 kV.). Particle size was obtained from counting 100 particles observed in SEM images.

2 Results and discussion

The XRD pattern of synthesized rod-like hydrated magnesium carbonate at 293.2 K is shown in Fig.1 (a). All the peaks can be indexed to the monoclinic crystalline phase of $MgCO_3 \cdot 3H_2O$, which is in good agreement with reference data(PDF 20-0669).

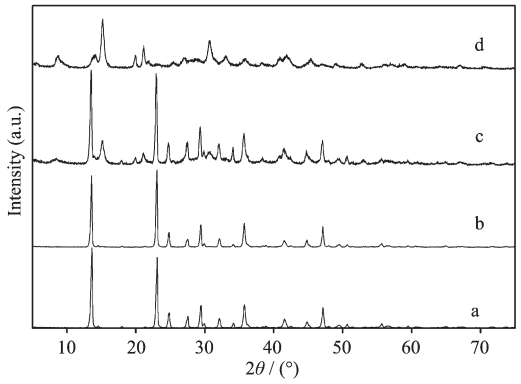

(a) nesquehonite precursors; (b) 20 min; (c) 40 min; (d) final product

Fig.1 XRD patterns of the products at different reaction times during pyrogenation process

The reaction followed by mixing $MgCl_2$ and Na_2CO_3 is a complex reactive crystallization process. The precipitation takes place and generates a large amount of primary nanoparticles initially. With the continuous stirring and the increase of reaction time up to about 14 min, a small number of micrometer-sized rod-like crystals or aggregates appear in the slurry serving as $MgCO_3 \cdot 3H_2O$ seeds. Under continuous stirring, there is no flocculation observed under microscope after 34 min, and it can be considered that it has been completely transferred into rod-like crystals. If the stirring ceases after 15 min, the system will no longer produce new seeds. A large quantity of primary nanoparticles exist in the system, which are gradually transferred into crystalline $MgCO_3 \cdot 3H_2O$ in the later aging time, grow onto the existing crystal particles to complete the ordering process and eventually grow into larger size rod-like $MgCO_3 \cdot 3H_2O$. The detail of the synthesis method was described in ref.[26]. Fig.2(a) shows the SEM images of synthesized $MgCO_3 \cdot 3H_2O$. It is obvious that the microrods are well crystallized with a length of 60~150 μm (the average length is 115 μm) and aspect ratio of 8.3~11.7 (the average aspect ratio is 10.4).

The stability of nesquehonite is between that of amorphous magnesium carbonate and hydromagnesite. Nesquehonite will transfer into hydromagnesite in aqueous solutions. The XRD pattern of the final spherical product is shown in Fig.1 (d). All the peaks in this Figure can be indexed to the monoclinic crystalline phase of $4MgCO_3 \cdot Mg(OH)_2 \cdot 4H_2O$ in agreement with reference data(PDF 25-0513).

As shown in Fig.2 (h), the final product is porous rosette-like, and most of them are composed of several spherical crystals growing together. If sunken parts and some incomplete growth areas appear on the surface, a "nest-like" shape will be presented. The actual morphology of hydromagnesite polycrystal is assembled by numberless two-dimensional slightly curly nano-sheets to make up of a structure as "house of cards". In order to reduce the surface energy, they gather into a ball. 100 particles in the SEM images are randomly selected to measure the spherical diameter D. The result shows that the spherical diameter is in the range of 30~60 μm and the average is 40 μm. In order to explore the evolution from nesquhonite microrods to hydromagnesite microspheres with rosette-like morphology, time-evolution experiments were carried out. SEM photos of particles at different stages of the pyrogenation process are shown in Fig.2 (b~h).

According to the work by Dong et al.[27], the dissolved nesquehonite can reach about 7.632 mmol·L^{-1} in 2 min when it is put into the water at 80 ℃ and

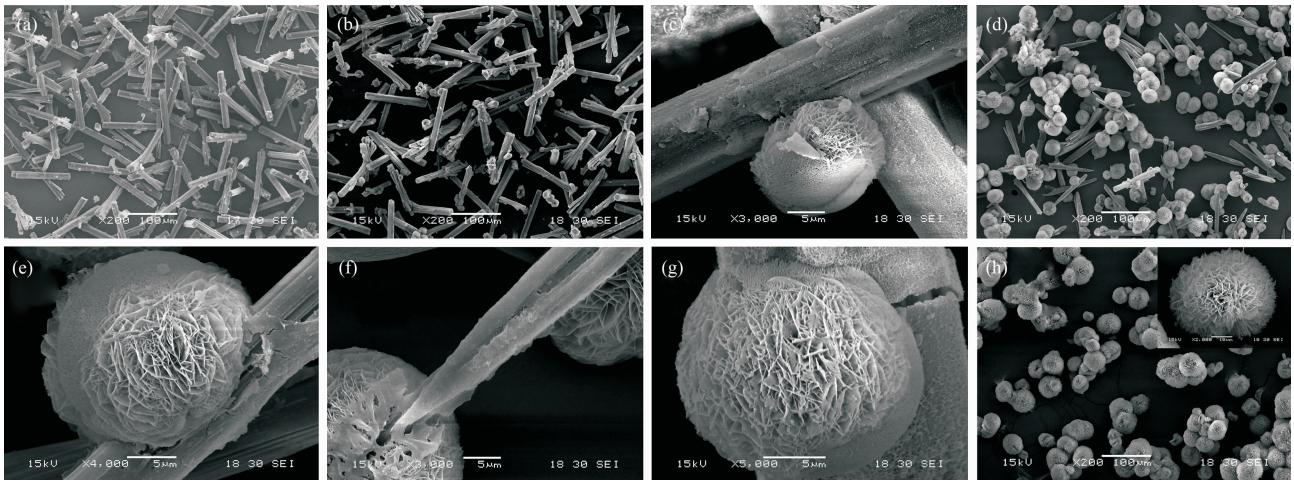

(a) the as-synthesized rod-like $MgCO_3 \cdot 3H_2O$; (b,c) at 20 min during pyrogenation process; (d,e,f,g) at 40 min during pyrogenation process; (h) hydromagnesite obtained by pyrogenation. The inset image is a typical hydromagnesite microsphere

Fig.2　SEM images of magnesium carbonate at different synthesis stages

the solubility of hydromagnesite is only about 0.937 4 mmol·L^{-1}[28]. The supersaturation ratio is about 1.82. Since the pyrogenation process is under static condition, the part close to the rod-like particle has relatively high local supersaturation due to the dissolution of $MgCO_3 \cdot 3H_2O$. Fig.2(b, c) shows the SEM images of nesquhonite undergoing the pyrogenation process for 20 min. In the panoramic image, some spherical or nest-like grains cling onto $MgCO_3 \cdot 3H_2O$ microrods sparsely. These grains "grow" on the rod side faces or tips, which is similar to mushrooms growing on tree trunks. Compared to the spherical shape, the particles are irregular, slightly flattened and sunken on many particles back (away from the rod). From the close-up image of an individual attachment, it is obvious that $MgCO_3 \cdot 3H_2O$ surfaces is rough as the same as chapped skin, which exhibits an interlocking network. These results are in good agreement with Dheillys[29]. The appendiculate grain has a typical surface of "house of cards" structure composed of $4MgCO_3 \cdot Mg(OH)_2 \cdot 4H_2O$ nano-sheets. It is interesting that the grain is divided into two hemispheres by a clear suture in the back. The hollow and the suture on the grains back mentioned above, to some extent, imply that the seed crystals of the basic magnesium carbonate are hatched from the rod-like particles. Once the spherical particles begin to grow, the growth speed is fast near the rod. Diffusion becomes an important factor in the growth dynamics.

With the extension of reaction time up to 40 min (Fig.2 (d ~g)), the "nutrient" (growth material) of the "tree trunk" (the nesquehonite microrod) is gradually absorbed by growing "mushrooms" (hydromagnesite growing on the microrod). The increase in the size of $4MgCO_3 \cdot Mg(OH)_2 \cdot 4H_2O$ microspheres is extremely obvious. Relatively, the $MgCO_3 \cdot 3H_2O$ micro-rods become shorter and thinner and both tips become needle-shaped due to dissolution while the surface exhibits rough peeling layer and grooves. There′s no existence of hollows on the back of spherical particles at this stage, which may be owing to their gradual growth in the pyrogenation process and their complete disappearance eventually. There are also some spherical particles growing together. One possibility is that local supersaturation makes the growth happen on both sides of the hemisphere, forming the aggregation of two spherical particles. Another one may be that several nuclei nucleate and grow at the binding site on nesquehonite microrods.

By carefully looking into the surface structure of the hydromagnesite particles at different pyrogenation stages, it is worth noting that the leaf-like crystallites become more compactly arranged on the particles surface when pyrogenation takes less time, in other words, there is larger amount of flakes per area unit. On the contrary, as the pyrogenation continues, the

arrangement becomes much looser. Moreover, the binding site of microspheres and microrods is a layer of substance, which is different from the main body of sphere and the body of nesquehonite micro-rods representing "batholith" (Fig.2 (g)). Therefore, it can be concluded that the growth of hydromagnesite starts from the binding site and grows outward. The leaf-like hydromagnesite accumulation pushes out the primal surface, which makes the structure of "house of cards" become loose gradually and ultimately "burst" into rosette-like hydromagnesite. The growth mode can be used to interpret many interesting phenomena in the pyrogenation process, such as the hollow on the back of sphere appearing at the 20th min and disappearing at the 40th min (it may have happened before this moment), which results from the growth of bottom crystallites.

The sunken parts and incomplete growth areas show the growth traces of $4MgCO_3 \cdot Mg(OH)_2 \cdot 4H_2O$. If the particle grows on the side face of the rod, the binding sites of the attachments and the substance nesquehonite rod will be arc-shaped and concave to the interior of spherical $4MgCO_3 \cdot Mg(OH)_2 \cdot 4H_2O$(Fig.2 (e)). As a result, a "nest" will come into being after the completion of growth to retain this trail. The section plane of the nest is oval-shaped. Similarly, the binding sites of the particles growing on the tip of $MgCO_3 \cdot 3H_2O$ microrod are small that a mini slit will be left on $4MgCO_3 \cdot Mg(OH)_2 \cdot 4H_2O$ when $MgCO_3 \cdot 3H_2O$ dissolves into a needle-like one. The slit is small and easy to be filled up in the following growth forming intact spherical particles. As shown in Fig.2 (f), some floccules can be observed. According to the research by Dong et al.[27], nesquehonite in aqueous solution will transfer into amorphous phase at high temperature. This is not reflected in the XRD patterns. This is due to the diffraction peaks of crystalline phase cover up the existence of amorphous. The characteristics of the system are that magnesium carbonate crystals are crystallized from amorphous nanoparticles. It is multi-step dynamic process and once local supersaturation is formed, amorphous phase forms firstly.

Fig.1 shows the XRD patterns of the product at different periods of time during the pyrogenation process. It is obvious that $MgCO_3 \cdot 3H_2O$ is gradually transformed into $4MgCO_3 \cdot Mg(OH)_2 \cdot 4H_2O$ as time goes by. As the diffraction peak intensity of $4MgCO_3 \cdot Mg(OH)_2 \cdot 4H_2O$ is much weaker than that of $MgCO_3 \cdot 3H_2O$, the diffraction peaks of $4MgCO_3 \cdot Mg(OH)_2 \cdot 4H_2O$ are concealed at the 20 min. Increasing the reaction time up to 40 min, a large amount of $4MgCO_3 \cdot Mg(OH)_2 \cdot 4H_2O$ appears to demonstrate its strong diffraction intensity that can clearly be identified.

Fig.3 shows the typical FTIR spectra of the particles obtained from different reaction times. It can be observed that the spectra change significantly with the increase of reaction time. For the precursor, the IR spectra are very similar to those of $MgCO_3 \cdot 3H_2O$, which are confirmed by the presence of 850 cm^{-1} (ν_2 mode), 1 105 cm^{-1} (ν_1 mode), 1 485 and 1 420 cm^{-1} (ν_3 mode) CO_3^{2-} adsorption bands. Different amounts of crystallization water give the broad bands in the range of 3 600~3 000 cm^{-1} and a faint band at about 1 645 cm^{-1} is associated with O-H bending mode. All these results indicate that the rod-like particles obtained below 293.2 K have a formula of $MgCO_3 \cdot xH_2O$, which is in good agreement with the results reported in the previous work[30,31].With the increase of reaction time up to 3 h (the reaction should be completed before this time), a great change takes place on the IR spectra. In contrast to the precursor, O-H bond appears in the crystalline water molecules and there is a sharp

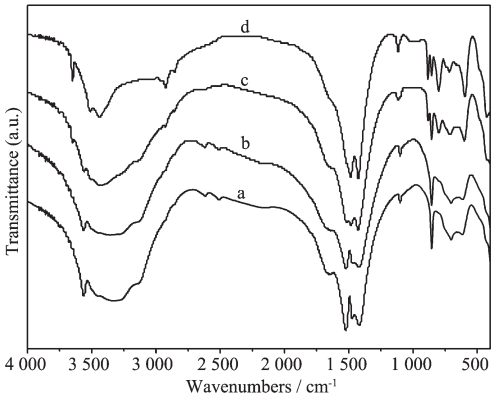

(a) nesquehonite precursors; (b) 20 min; (c) 40 min; (d) final product

Fig.3 FTIR spectra of products at different reaction time during pyrogenation process

band around 3 650 cm^{-1} corresponding to the free O-H vibration. Moreover, the bands between 3 600 and 3 400 cm^{-1} also become narrower. As $4MgCO_3 \cdot Mg(OH)_2 \cdot 4H_2O$ consisting of more CO_3^{2-} groups, the carbonate bending vibrations split into three absorption bands at 800 (the strongest), 850, and 880 cm^{-1}. All of the features are suggested as the characteristic adsorption of $4MgCO_3 \cdot Mg(OH)_2 \cdot 4H_2O$, which is consistent with the XRD results.

A challenge in materials engineering is to make the controlled assembly of purposely designed molecules or ensembles of molecules into different scales with special properties and functions. Due to restrictions of the crystal habit, it is tremendously difficult to achieve the desired architectures. However, there is a dramatic change of morphology on the raw materials and desired products in our experiments.

Fig.4 shows the schematics of the hydromagnesite microspheres growth process. Crystallization is a multi-step dynamic process, rather than a one-step thermodynamic process. Amorphous precursor particles are favored to form as the first species at high supersaturations according to the Ostwald rule of stage. When the precipitation begins, amorphous nanoparticles initially form from the mixture solution (Fig.4a), and then they tend to quickly aggregate together to form larger, more thermodynamically stable particles, which affect the size and shape of final samples. With the extension of reaction time, the morphology of the synthesized samples varies from particles to microrods (Fig.4b). Finally, all particles are changed into microrods with uniform diameter distribution (Fig.4c). At

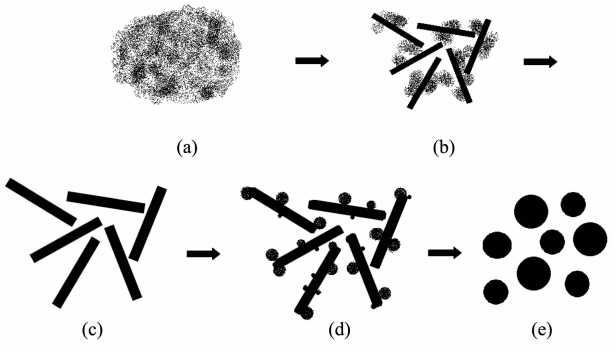

Fig.4 Schematics of the hydromagnesite microspheres synthesis and growth process

353.2 K, the dissolution of $MgCO_3 \cdot 3H_2O$ forms local supersaturation which again leads to the generation of amorphous precursor particles. According to the view of Cölfen et al.[32], the formation of amorphous precursors and crystallization of inorganic salt belong to the non-classical crystallization process. Driven by thermodynamics, by oriented attachment and fusion, these nanoparticles shape nano-leaf $MgCO_3 \cdot Mg(OH)_2 \cdot 4H_2O$ crystallites growing on the surface of $MgCO_3 \cdot 3H_2O$ microrods (Fig.4d). The microrods disappear and microspheres form at last (Fig.4e). The balance between the dissolution rate of nesquehonite and the deposition rate of hydromagnesite is considered to be a dynamic factor in the process of microspheres formation. The involved processes and mechanism during pyrogenation may be as follows: ($MgCO_3 \cdot 3H_2O$) dissolution-amorphous particles formation-($4MgCO_3 \cdot Mg(OH)_2 \cdot 4H_2O$) crystallization.

3 Conclusions

In this work, a multi-step chemical conversion strategy to achieve the indirectly synthesis of desired architectures was developed. Porous rosette-like $4MgCO_3 \cdot Mg(OH)_2 \cdot 4H_2O$ was obtained by the pyrogenation of $MgCO_3 \cdot 3H_2O$. Because of the mild reaction condition without introducing additives, products with high purity can be prepared. The transformation from $MgCO_3 \cdot 3H_2O$ microrods to the $4MgCO_3 \cdot Mg(OH)_2 \cdot 4H_2O$ microspheres can be moused out from the transition state in the process. During the pyrogenation process, $MgCO_3 \cdot 3H_2O$ crystals dissolve and $4MgCO_3 \cdot Mg(OH)_2 \cdot 4H_2O$ crystals grow. Amorphous substance may form firstly due to local supersaturation. The nanoparticles crystallize into hydromagnesite microcrystals forming rosette-like morphology finally. Some phenomenon such as the formation of nest-like particles can be explai ned according to the mechanism mentioned above.

References:

[1] Yan C, Xue D, Zou L, et al. *J. Cryst. Growth*, **2005**,**282**(3/4): 448-454

[2] Rasenack N, Müller B W. *Int. J. Pharm.*, **2002**,**244**(1/2):45-57
[3] YANG Juan-Yu(杨娟玉), LU Shi-Gang(卢世刚), KAN Su-Rong(阚素荣), et al. *Chinese J. Inorg. Chem.* (*Wuji Huaxue Xuebao*), **2009**,**25**(4):756-760
[4] WANG Feng(王峰), WANG Qiu-Shi(王秋实), CUI Qi-Liang(崔启良), et al. *Chinese J. Inorg.Chem.* (*Wuji Huaxue Xuebao*), **2009**,**25**(6):1026-1030
[5] Mann S. *Angew. Chem. Int. Ed.*, **2000**,**39**(19):3392-3406
[6] Fang X S, Yoshio B, Liao M Y, et al. *Adv. Mater.*, **2009**,**21**(20):2034-2039
[7] Fang X S, Bando Yoshio, Gautam U K, et al. *J. Mater. Chem.*, **2008**,**18**(5):509-522
[8] Fang X S, Xiong S L, Zhai T Y, et al. *Adv. Mater.*, **2009**,**21**(48):5016-5021
[9] Clfen H, Qi L, Mastai Y, et al. *Cryst. Growth Des.*, **2002**,**2**(3):191-196
[10]Wang T, Cölfen H. *Langmuir*, **2006**,**22**(21):8975-8985
[11]Mitsuhashi K, Tagami N, Tanabe K, et al. *J. Photochem. Photobiol. A*, **2007**,**185**(2/3):133-139
[12]Zhang Z, Zheng Y, Zhang J, et al. *J. Chromatogr. A*, **2007**, **1165**(1/2):116-121
[13]Russell M J, Ingham J K, et al. *J. Geol. Soc.*, **1999**,**156**(5):869-888
[14]Zhang Z, Zheng Y, Chen J, et al. *Adv. Funct. Mater.*, **2007**, **17**(14):2447-2454
[15]Hao Z, Pan J, Du F. *Mater. Lett.*, **2009**,**63**(12):985-988
[16]Mitsuhashi K, Tagami N, Tanabe K, et al. *Langmuir*, **2005**, **21**(8):3659-3663
[17]Ohkubo T, Suzuki S, Mitsuhashi K, et al. *Langmuir*, **2007**, **23**(11):5872-5874
[18]ZHANG Li-Li(张黎黎), LIU Jia-Xiang(刘家祥), LI Min(李敏). *J. Chin. Chem. Soc.*(*Guisuanyan Xuebao*), **2008**,**36**(9):1310-1314
[19]Cheng W T, Li Z B, George P D. *Chin. J. Chem. Eng.*, **2009**, **17**(4):661-666
[20]Cheng W T, Li Z B. *Ind. Eng. Chem. Res.* **2010**,**49**(4):1964-1974
[21]Zhang Z, Zheng Y, Zhang J, et al. *Cryst. Growth Des.*, **2007**, **7**(2):337-342
[22]Yan C, Xue D. *J. Phys. Chem. B*, **2005**,**109**(25):12358-12361
[23]Li Q, Ding Y, Yu G, et al. *Solid State Commun.*, **2003**,**125**(2):117-120
[24]Liu F, Sun C, Yan C, et al. *J. Mater. Sci. Technol.*, **2008**,**24**(4):641-648
[25]Hänchen M, Prigiobbe V, et al. *Chem. Eng. Sci.*, **2008**,**63**(4):1012-1028
[26]SONG Xing-Fu(宋兴福), YANG Chen(杨晨), et al. *CN Patent*, 101830488 A, **2010**.
[27]Dong M, Cheng W, et al. *J. Chem. Eng. Data*, **2008**,**53**(11):2586-2593
[28]Cheng W T, Li Z B. *Ind. Eng. Chem. Res.*, **2010**,**49**(4):1964-1974
[29]Dheilly R M, Bouguerra A, Beaudoin B, et al. *Mater. Sci. Eng. A*, **1999**,**268**(1/2):127-131
[30]Botha A, Strydom C A. *J. Therm. Anal. Calorim.*, **2003**,**71**(3):987-995
[31]Zhang Z, Zheng Y, Ni Y, et al. *J. Phys. Chem. B*, **2006**,**110**(26):12969-12973
[32]Cölfen H. *Mesocrystals and Nonclassical Crystallization*. England: John Wiley & Sons, Inc., **2008**:75-78